

Comparison of geomatic techniques for rockfall monitoring

M. Amparo Núñez-Andrés¹, Felipe Buill¹, Càrol Puig¹, Nieves Lantada¹, Albert Prades¹, Marc Janeras^{1,2}, Josep A. Gili¹

¹Universitat Politècnica de Catalunya, Civil and Environmental Department, Barcelona, Spain, ²Institut Cartogràfic i Geològic de Catalunya, Barcelona, Spain

m.amparo.nunez@upc.edu, felipe.buill@upc.edu, carol.puig@upc.edu, albert.prades.i@upc.edu, nieves.lantada@upc.edu, marc.janeras@icgc.cat, j.gili@upc.edu

Key words: *Rockfall; geomatic techniques; Terrestrial Laser Scanning TLS; Terrestrial and UAV photogrammetry*

ABSTRACT

Rockfalls are slope instabilities very frequent and harmful in mountainous areas. They cause damage in infrastructures (roads and railways), buildings, vehicles and people. Several tests were carried out to understand better these events. The field activities comprised real scale tests and the characterization of natural events in the N-E of Spain, mainly in the Pyrenees range. Moreover, in order to understand the behaviour of the blocks during the fall real scale tests were carried out. We dropped a total of 124 rock blocs under controlled conditions. Prior to the block release and during their propagation downslope, several geomatic techniques were used to monitor the volumes, shapes and trajectories of the original blocks and their fragments (due to breakage); it is worth to highlight the videogrammetry to determine the trajectories of the blocks. In order to survey the natural rock walls, source of the rockfalls, the so-called massive data capture by photogrammetry (both terrestrial and UAV-drone with image and video) and Terrestrial Laser Scanning (TLS) have been used, in this way the different techniques can be compared. Finally, for the monitoring of some rock cliffs, with recurrent rockfalls, the TLS was used, trying to catch some precursory displacements that may help in the risk management of the areas at the bottom. In our contribution, the aforementioned geomatic techniques (videogrammetry, photogrammetry – terrestrial or aerial –, and TLS) are combined and compared, highlighting the pros and cons of the different methods and their applications according to environmental conditions.

I. INTRODUCTION

In the last decades geomatics techniques are being widely applied in geological and geomorphological applications.

The data and techniques cover a wide range: the use of historical photographs obtained in cartographic photogrammetric flights (Bennett et al., 2012), photogrammetry from airplane and UAV (Unnamed Aerial Vehicle) (Eisenbeiß et al., 2005) (Aicardi et al., 2017) (Tziavou et al., 2018) (Niethammer et al., 2012; Stumpf et al., 2013), satellite images (Liberti et al., 2009) or with laser scanning, terrestrial (TLS) or aerial (ALS) (Jaboyedoff et al., 2012) (Bremer and Sass, 2012) (Gigli et al., 2014), figure 1. Each of the techniques presents small variations in their own methodology and instrumentation, for example, the capture of stereoscopic images can be done by taking photographs or video and then extracting the frames with the appropriate overlapping to build a 3D model.

Likewise, each one of these techniques presents advantages and disadvantages, both of completion and accuracy of models, as well as differences in time and cost of execution. The geomatics terrestrial techniques of 3D data capture, photogrammetric or LiDAR (Light Detection and Ranging), present the same disadvantages; the most important is the occlusion of

part of the elements that are hidden by others due to the perspective. This is solved with an aerial shot that until relatively recently supposed a significant increase in the economic cost, but nowadays they are widely extended with the use of UAV platforms for the transport of cameras and laser scanner sensors.

Geomatic techniques allow accurate 3D models without having to get too close to the study area, which is very useful as they are often unstable and dangerous areas. We must bear in mind that the farther we are, the lower quality the resulting model will be. Nowadays these techniques are present in most of the studies.

The majority of the obtained models are used to measure volume changes or displaced mass after an event. In this paper, we focus in rockfalls, showing the comparison of different techniques for the characterization of the rock mass and the use of some methodologies to analyse the behaviours of the blocks during the fall in controlled in-situ test.

Due to the nature of this kind of phenomena, techniques that capture data from the nadir position, (aerial photogrammetry, high altitude ALS or satellite image) are not useful to detect and measure the source zones since they are vertical rock walls (only partially visible from the nadir).

Additionally, the rock escarpment models may provide information of the existence of cracks and

joints, which control the rockfalls occurrence and volume, i.e. to characterize the predominant failure mechanism from the analysis of detachment scars and holes in the surface of the cliff.

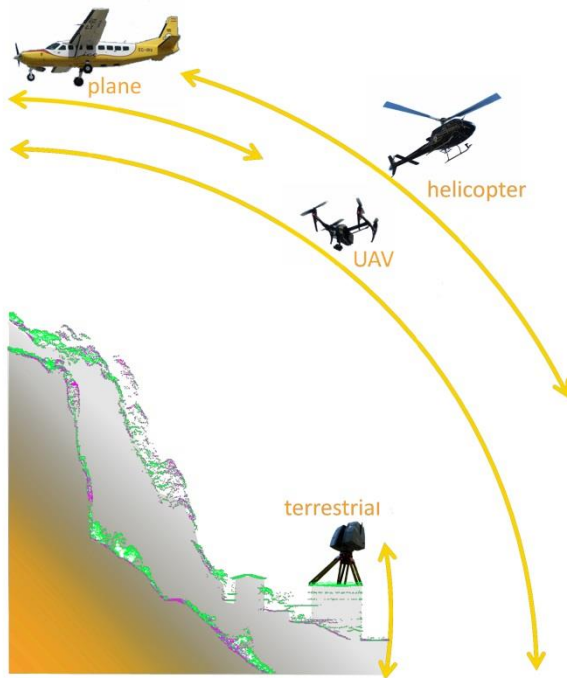


Figure 1. Different geomatic techniques and platforms to capture 3D information (modified from Janeras et al., 2018a).

Information about the trajectories of the blocks during the fall and the kinetic energy of these blocks, (and/or their fragments in case of breakage) could be obtained from the information gathered during the in-situ test. To describe the trajectories, it is necessary to have a previous DTM as a reference.

All this knowledge allows establishing future remedial measures (prevention and/or protection).

In next sections we will describe the photogrammetric techniques, with photos and video, used not only for the characterization of the rock walls but also for the block tracking during the field experiments. Moreover, we will describe the use of TLS to detect premonitory deformations of rockfalls or to estimate the detached rock volume.

II. TEST SITE

The real scale tests shown in this paper were carried out in different sites, regarding the technique and methodology to employ.

The photogrammetric tests using photography and video were carried out in quarries.

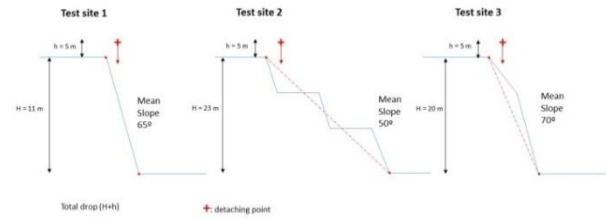


Figure 2. Sections of the different test site in quarries.

Also the drop tests were carried out in several quarries in order to have controlled conditions. The lithology was different in each case; this matters when the blocks impact directly over the bedrock. The section in each quarry was slightly different, as shown in figure 2. The blocks were granite, massive limestones and dacites and the fall heights were around 16 m, 28 m and 25 m respectively. This value includes the height of the mechanical loader that rose the block for the dropping (Gili et al., 2016).

III. METHODOLOGY

The different techniques described in this section were used in the fragmentation test and in the survey for obtaining the DTM.

A. Videogrammetry

As we have mentioned above, one of the objectives of the project was to improve the knowledge of rock fragmentation.

To be more specific about what we want to study the following questions could be asked: how often does the fragmentation happen? Do limits of energy exist that guarantee the fragmentation of a block? What are the values of the coefficient of restitution in a specific substrate?

To check these issues, a total of 124 blocks were dropped in three different quarries, with volumes ranging from 0.2 to 4.3 m³.

Before the dropping, a photogrammetric survey for each block was carried out. The coordinates of several targets were used for the computation of external orientation parameters in the photogrammetric process.

The trajectories during the fall were recorded with three high speed video-cameras synchronized using a flash light.

The centre of mass of each block, extracted from the block photogrammetric survey, was projected into the image to follow the body during its propagation downslope, enabling the extraction of dynamic and kinematic parameters.

In order to compute the inertial tensor vector the method described in Blow and Binstock (2004) was used. Once the block position can be computed in terrain coordinates, figure 3, in each moment, the velocity in the trajectory can be computed considering the time between images shots. With the frames before and after the impact the initial and final velocity is

computed, and also the restitution coefficients for the point of impact (Asteriou et. al., 2012). Since the mass of the block is known we computed the kinetic energy before and after the impact and so the energy lost during the impact may be established.

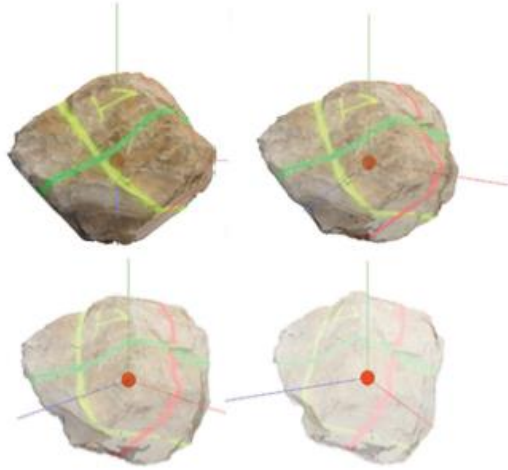


Figure 3. Site1, Block 1 3D model, where the centre of mass is positioned from four points of view.

This geometric information (terrain, block, gravity centre, structure) is very important for the modelling of trajectories and fragmentation patterns. Using convergent video capture, after the scene is orientated from targets, the positions of the block (and its fragments) along the trajectory can be triangulated, obtaining velocities (figure 4 shows the components of velocity), acceleration, energy, etc (Prades et al., 2017). For example, the impact velocities against the floor have a range between 12.5 to 16.9 m/s, depending the specific scenario.

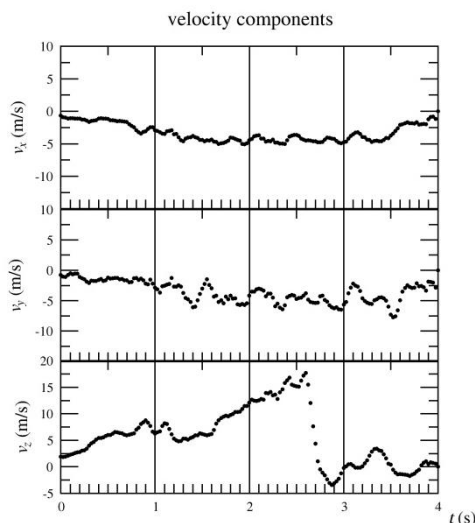


Figure 4. Example of the velocity components (m/s) function of time (s).

B. Photogrammetry: image or video

The use of unmanned aerial vehicles (UAV) to capture the images has made easier and cheaper the aerial photogrammetric process. In this way the occlusions, due to the relief or vegetation, are avoided.

The photographic cover can be planned easily and the photographs taken faster than using an aeroplane. Moreover, the possibility of taking oblique and nadiral photographs allows covering the terrain even if it is escarped. Another advantage is the proximity to the object since the captured detail is sufficient for the geological analysis. Additionally, large focal length can be used since the UAV camera has a very stable behaviour thanks to the gimbal.

In parallel the use of SfM algorithms (Structure from Motion) to obtain 3D models has allowed the use of non-metric and low-cost cameras with accurate results in geological applications. Moreover, these cameras allow capturing videos with enough quality to build 3D models from their frames.

Several studies show the comparison between results obtained using different techniques (Lato et al., 2015), different cameras taking as ground truth the TLS model (Thoeni et al., 2014) or different software (Gómez-Gutiérrez et al., 2015). Figure 5 shows the models obtained using photogrammetry and TLS of the Olorda quarry.

In this study, we have analysed the differences among models using different cameras and taking photography and video from UAV and from ground. The differences were established not only in geometry, but also we have analysed the quality from the point of view of completeness.

Two similar cases are shown, first a rockwall with dimensions of 100 m in length, 80 m depth and a height difference of 75 m. In the second, the dimensions were of 200 m length and a height from 10 to 70 m.

In the terrestrial photogrammetry case, the camera was a Canon EOS 450D, with a 3/2 CMOS sensor of 12.2 Mpx (4272x2848) and a lens SIGMA Aspherical with fixed focal length 24 mm and aperture f/1.8 EX DG. To avoid the effect of the sun illumination in the images (shadows, excessive contrasts, hidden details...) the HDR technique (High Dynamic Range) was used.

The aerial coverage was taken from a quadcopter DJI Inspire 1 Pro 4K with a camera, cardan/gimbal system and a GNSS receiver. The camera is a Zenmuse X5 model FC550 with a sensor 4/3 CMOS of 16 Mpx (4608x3456), the lens is DJI MFT model with focal length 15 mm, aperture f/1.7 and aspherical lens (ASPH). Moreover, it has the possibility to capture 4K video (4096x2160) that in this case was used to 23 fps and a field of view (FOV) of 94°.

In the first study area, the images were taken from an average height of 30 m for the photogrammetric survey and from 26 to 32 m in the case of video, so the scale is between 1/2250 and 1/1700. In the second case the average distance in the photographic capture was of

48 m for the picture and 52 m for the video, so the photographic scale was in the range of 1/3200 and 1/3500, respectively.

Control points appear in all the acquired images. They were targets, when possible, or well identified natural points. These points are essential, not only for the georeferencing, but also to correct alignment errors among point clouds that form the model (Thoeni et al., 2014).

In both cases, the photogrammetric process was carried out with Agisoft (Agisoft, 2016). Individual and combined models were built. In this last set, the models were computed using a terrestrial and aerial photographs coverage, and a terrestrial photographs and video coverage.

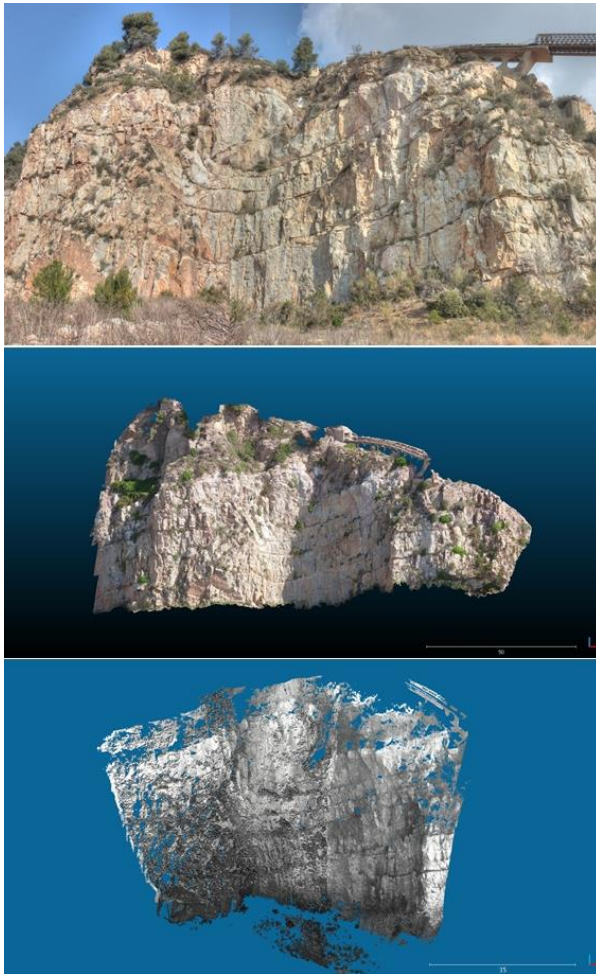


Figure 5. From top to bottom, picture, photogrammetric model and TLS model of the Olorda quarry

The characteristics of the models are shown in table 1 and 2, for the case zones 1 and 2, respectively.

Table 1. Case 1. Characteristics of the models Terrestrial (T), Aerial Photogrammetry (AP), Aerial Video (V) and their combinations.

	T	AP	V	T + AP	T + V
Nº Images	91	316	323	407	414
GSD (m)	0.005	0.008	0.006	0.008	0.006
MDT (Pts/m ²)	2476	1074	1698	1013	1964
σ X (m)	0.005	0.004	0.010	0.009	0.013
σ Y (m)	0.011	0.013	0.005	0.013	0.011
σ Z (m)	0.011	0.012	0.016	0.010	0.020

Table 2. Case 2. Characteristics of the models Terrestrial (T), Aerial Photogrammetry (AP), Aerial Video (V) and their combinations.

	T	AP	V 4k	T + AP
Nº Images	107	669	186	776
GSD (m)	0.010	0.013	0.012	0.012
Nº points MDT	8.35 M	18.32 M	7.60 M	26.18 M
σ x (m)	0.018	0.015	0.008	0.019
σ y (m)	0.014	0.017	0.017	0.020
σ z (m)	0.024	0.031	0.010	0.027

Techniques comparison

On the one hand, the aerial images avoid the occlusion in some areas. On the other hand, the use of terrestrial images allows the clearest identification of the control points since the photographs were taken from the same point of view that the points which were measured with total station.

In the terrestrial photographic case, with the use of the HDR technique an improvement in the quality of the image was observed as well as a greater number of correlated points.

Regarding the use of 4K video, it can be concluded that it would be at the same level of quality as the conventional photographic shot for most of the cases. The obtained models have the same resolution and precision after extracting the frames with adequate overlap from these videos.

The model obtained from terrestrial photogrammetry is not complete due to the occlusions. In order to improve the completeness a complementary survey from a UAV platform can be done.

Eventually, the model obtained with TLS is similar to the terrestrial photogrammetric one, with a more

homogenous resolution, since in the photogrammetric model we can find areas where the correlation is not possible.

The ideal way of obtaining models with these techniques would be the combined use of a terrestrial technique and the aerial survey with UAV platform. In this way, the non-accessible areas are completed. Regards the costs, photogrammetry is more competitive than laser scanning techniques.

C. Terrestrial Laser Scanning

The TLS is another of the techniques widely used in the landslide and rockfalls monitoring. Although always advisable (to obtain a high resolution and precision for instance), to be physically close to the slope, according to the circumstances, may be impossible, difficult and/or dangerous.

Periodic campaigns are carried out to monitor multi-temporal variations and deformations. These campaigns have a double purpose. On one hand, the detection of rockfalls comparing point clouds. On the other hand, the rock wall deformation that can indicate future movements. With the TLS we obtained point clouds, from which we can perform differential analysis that will lead to the estimation of volume loss, deformations or small movements triggering collapse (fig. 6). Moreover, the differences among the models, mainly if the measurement is in continuous mode, can give us warnings on current deformations, which can be the precursor of an approaching avalanche (Adam et al., 2014).

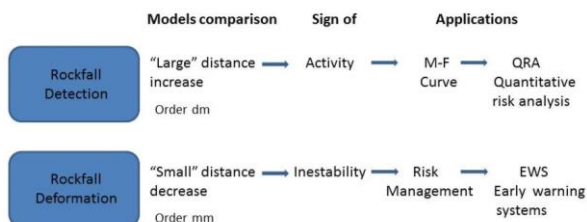


Figure 6. TLS role in Rockfall Detection and Deformation

Two examples are shown in table 3. In both of them a sensor ILRIS-3D Optech was used. In the first case, small deformations cannot be detected. In the second one these changes enabled detection in some areas.

The first case is a protected natural space located in the central Iberian Range, NE Spain, a NW-SE trending alpine intraplate fold belt. The limestone and dolomite rocks outcropping at the river gorge are highly resistant materials that form vertical slopes of more than a hundred meters high (Corominas et al. 2019).

The study area was scanned the first time in 2017 and since then up to present (February 2019) it has been monitored twice per year to follow its evolution and activity. The total length of the scanned wall is 1 km with a height from 40 m to 100 m. The scanning distance varies from 100 m to 150 m with Ground Sample

Distance (GSD) of 2.7 cm. The cliff has been divided into sectors, which present homogeneous conditions (bedding orientation) related to the stability.

The processing steps were: removal of the vegetation; alignment of each cloud with respect the first data set with the iterative closest point (ICP) algorithm (Chen and Medioni, 1991); identification and masking of areas-of-change; reapplication of the ICP algorithm; and, finally, calculation of differences between two consecutive campaigns.

In this case, it has been possible to detect and calculate the volume of rockfalls (figure 7) but precursory movements were not detected. Perhaps the displacements were smaller than the precision of the monitoring setup; or the blocks under movement fell before the next campaign arrived.

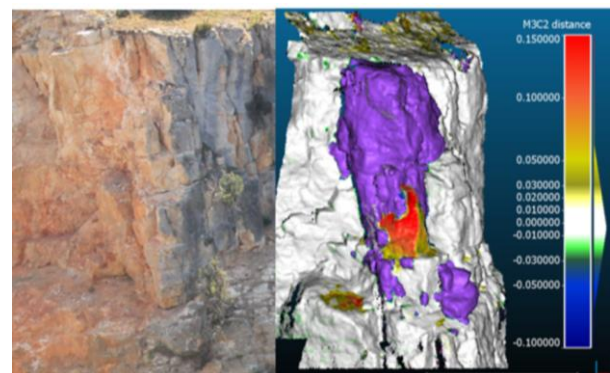


Figure 7. TLS, Case 1. Left: picture of a rockfall detected between two campaigns. Right: volume loss of 28 m³ (purple) and displacement of the rock (red).

The rockfall volume of each block detached has been calculated comparing the 3D point clouds of two successive campaigns. The results obtained for this case study supplement the magnitude-frequency (M-F) relation of rockfall events at the site. All this information is the input data to carry out the quantitative risk analysis (QRA), (Corominas et al. 2019).

To calculate the probability of the rockfall event reaching the exposed humans and infrastructures, the GIS-based code RockGIS was used. This program, developed by the group, simulates stochastically the trajectories of the blocks taking into account their fragmentation (Matas et al. 2017). The input data for RockGIS are the land use map and the digital surface model (DSM), the rockfall sources and their volumes obtained from the TLS point cloud.

The second case corresponds to Montserrat Mountain (Catalonia, Spain), a huge conglomerate massif where monitoring surveys have been carried out since 2007 with a variety of techniques. As a concurrent example for this contribution, Figure 8 shows different pictures depicting a progressive failure detected with TLS.

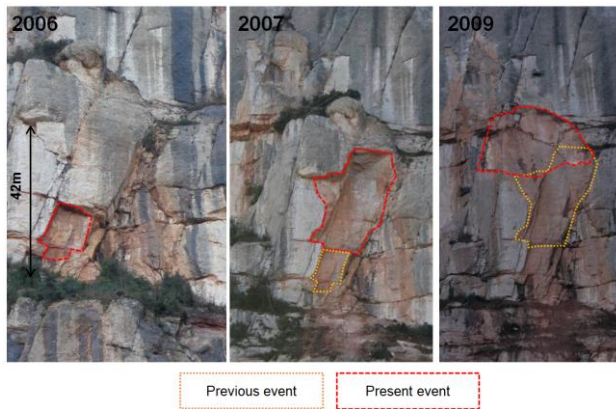


Figure 8. TLS, Case 2. Degotalls wall. Rockfall sequence interpreted as a progressive failure causing partial detachments, which were detected with TLS (May 2007 and December 2009) (modified from Janeras et al. 2018b).

The use of different techniques in the campaigns sometimes can cause interferences among them. For example, the prisms for the measurement with total station interfere the normal operation of the TLS because the huge change in reflectivity mask the ground around the prism; eventually, the TLS sensor may be damaged due to the high intensity on the laser return.

In this Case 2, the average scanning distance was 250 m. In order to cover the intended cliffs, 10 stations and 22 scans were need. After the data acquisition, the points were reclassified using the software CANUPO (Brodu and Lague, 2012), in order to remove the vegetation. Then, the point clouds were merged and registered (Janeras et al. 2017).

Table 3. Characteristics of the TLS Case 1 and 2.

	Case 1	Case 2
Lithology	Limestone and dolomite	Conglomerate
Sector to be monitored	15	7
Number of campaigns	5	Up to 4/year (total 25 in Degotalls)
Years	2017-2019	2007-2019
Detection instabilities	2-3 cm	1-2 cm

After the point cloud registration, the multi-temporal comparison can be done (figure 9), taking one of them as a reference. In order to improve the results, the Nearest Neighbour filter is used, in this way the value for the detectable deformation becomes of 1 cm, close to the noise of the measurement. In this Case 2, it was possible to detect precursory movements of rockfalls in two blocks, both of them in the “Degotalls” sector, with initial displacements larger than 2 cm (Fig.9).

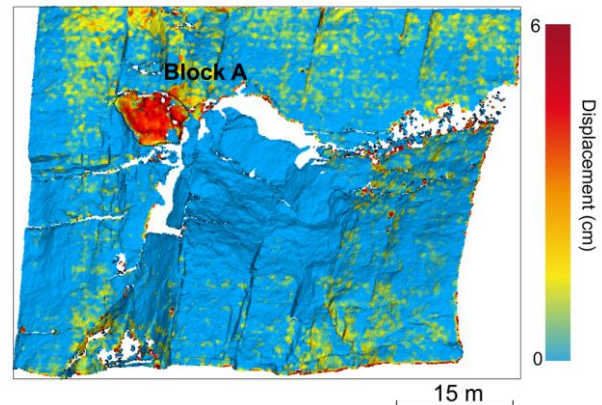


Figure 9. Case 2. Degotalls wall. Result of TLS monitoring. Example of movement detection comparing TLS campaigns.

IV. CONCLUSION

Geomatic techniques can be used both for continuous monitoring and for measurement after an event.

All these techniques allow us to obtain models with enough quality for geological applications. The combined use of methodologies allows us to cover a wide spectrum, both dynamic and static. For this reason they are useful in all the steps of a rockfalls analysis, from the measurement to establish the static conditions of the rock wall until the rockfall deposit.

The use of drones allows easy access to difficult and dangerous areas, obtaining 3D models even in areas with escarped terrain thanks to the versatility of the camera and gimbal.

Moreover, the use of high-speed video cameras has enabled the capture of high-quality information of inestimable value for the subsequent analysis of block launch events and their possible fragmentation in the real scale tests.

V. ACKNOWLEDGEMENTS

This study was partially supported by the research project “Characterization and modelling of rockfalls, RockModels” (Ref.BIA2016-75668-P)” funded by the Spanish Ministry of Economy and Competitiveness and co-funded by AEI/FEDER.UE.

References

- Adams, M., Bauer, A., Paar, G. (2014). Monitoring snow avalanche terrain with Automated Terrestrial Laser Scanning. In: *Proc of International Geoscience and Remote Sensing Symposium (IGARSS)*. pp. 4006-4009. 10.1109/IGARSS.2014.6947364.
- Agisoft (2016) Agisoft PhotoScan Professional Guides, available at <http://www.agisoft.com/>
- Aicardi, I., Dabove, P., Lingua, A., Piras, M. (2017). Integration between TLS and UAV Photogrammetry Techniques for Forestry Applications. *IForest*, Vol. 10 No. 1, pp. 41-47. <https://doi.org/10.3832/ifor1780-009>.

- Asteriou, P., Saraglou, H., Tsiambaos, G. (2012). Geotechnical and kinematic parameters affecting the coefficient of restitution for rockfall analysis. *International J. of Rock Mechanics and Mining Sciences*, Vol. 5, pp. 103-113.
- Bennett, G. L., Molnar, P., Eisenbeiss, H., Mcardell, B.W. (2012). Erosional Power in the Swiss Alps: Characterization of Slope Failure in the Illgraben. *Earth Surface Processes and Landforms*, Vol.37, No.15, pp. 1627–40. <https://doi.org/10.1002/esp.3263>.
- Blow, J., Atman J. (2004). How to find the inertia tensor (or other mass properties) of a 3D solid body represented by a triangle mesh. Internal document at: [http:// number-one.com/blow/inertia/bb_inertia.doc](http://number-one.com/blow/inertia/bb_inertia.doc) [2017].
- Bremer, M., Sass, O. (2012). Combining Airborne and Terrestrial Laser Scanning for Quantifying Erosion and Deposition by a Debris Flow Event. *Geomorphology*, Vol. 138, No. 1. pp. 49–60. <https://doi.org/10.1016/j.geomorph.2011.08.024>.
- Brodu, N., Lague, D. (2012). 3D Terrestrial Lidar Data Classification of Complex Natural Scenes Using a Multi-Scale Dimensionality Criterion : Applications in Geomorphology. *ISPRS Photogrammetry and Remote Sensing*, Vol. 68, pp. 121-134.
- Chen, Y., Medioni, G. (1991). Object Modeling by Registration of Multiple Range Images. In: *Proc. of IEEE International Conference on Robotics and Automation* (pp. 2724–2729). Sacramento, California.
- Corominas, J., Matas, G., Ruiz-Carulla, R. (2019). Quantitative analysis of risk from fragmental rockfalls. *Landslides*, Vol. 16, No. 1, pp 5–21 <https://doi.org/10.1007/s10346-018-1087-9>
- Eisenbeiß, H., Karsten L., Sauerbier, M. (2005). Photogrammetric Recording of the Archaeological Site of Pinchango Alto (Palpa, Peru) Using a Mini Helicopter (UAV). In: *Proc. of Annual Conference on Computer Applications and Quantitative Methods in Archaeology CAA*, Figueiredo A. (eds), 21–24. Tomar. http://www.photogrammetry.ethz.ch/general/persons/karsten/paper/eisenbeiss_et_al_2007.pdf.
- Gigli, G., Morelli, S., Fornera, S., Casagli, N., 2014. Terrestrial laser scanner and geomechanical surveys for the rapid evaluation of rockfall susceptibility scenarios. *Landslides*, Vol. 1, pp. 1–14.
- Gili, J.A., Ruiz, R., Matas, G., Corominas, J., Lantada, N., Núñez, M.A., Mavrouli, O., Buill, F., Moya, J., Prades, A., Moreno, S. (2016) Experimental study on rockfall fragmentation: In situ test design and first results. In: *Proceed. 12th Int. Symp. on Landslides*, June 2016, Napoli (Italy). Aversa et al. (Eds). pp: 983-990.
- Gómez-Gutiérrez, A., Sanjosé-Blasco, J.J., Lozano-Parra, J., Berenguer-Sempere, F., Matías-Bejarano, J. (2015). Does HDR Pre-Processing Improve the Accuracy of 3D Models Obtained by Means of two Conventional SfM-MVS Software Packages? The case of the corral del veleta Rock Glacier. *Remote Sens.*, Vol. 7, pp. 10269-10294.
- Jaboyedoff, M., Oppikofer, T., Abellán, A., Derron, M., Loye, A., Metzger, R., Pedrazzini, A. (2012). Use of LIDAR in Landslide Investigations: A Review. *Natural Hazards*, Vol. 61, No. 1, pp. 5–28. <https://doi.org/10.1007/s11069-010-9634-2>.
- Janeras, M., Jara, J.A., Royan, M.J., Vilaplana, J., Aguasca, A., Fabregas, X., Gili, J.A., Buxó, P. (2017) Multi-technique approach to rockfall monitoring in the Montserrat massif (Catalonia, NE Spain). *Engineering Geology*, Vol. 219, pp. 4-20 DOI: 10.1016/j.enggeo.2016.12.010
- Janeras, M., Gili, J.A., Palau, J., Buxó, P. (2018a) Checking the complementarity of different LiDAR / photogrammetry terrain models for rockfall mitigation in a demanding environment. In: 3rd Virtual Geoscience Conference (VGC-2018) proceedings, Kingston (Canada), August 2018. DOI: 10.13140/RG.2.2.31332.01922.
- Janeras, M., Gili, J.A., Guinau, M., Vilaplana, J.M., Buxó, P., Palau, J. (2018b) Lessons learned from Degotalls rock wall monitoring in the Montserrat Massif (Catalonia, NE Spain). In: 4th Rock Slope Stability Symposium (RSS-2018) proceedings, Chambéry (France), November 2018.
- Lato, M., Hutchinson, D.J., Gauthier, D., Edwards, T., Ondercin, M. (2015). Comparison of airborne laser scanning, terrestrial laser scanning, and terrestrial photogrammetry for mapping differential slope change in mountainous terrain. *Can. Geotech. J.*, Vol. 52, pp. 129–140.
- Liberti, M., Simoniello, T., Carone, M. T., Coppola, R., D’Emilio, M., Macchiato, M. (2009). Mapping Badland Areas Using LANDSAT TM/ETM Satellite Imagery and Morphological Data. *Geomorphology*, Vol. 106, No. 3–4. <https://doi.org/10.1016/j.geomorph.2008.11.012>.
- Low, J., Binstock, A. (2004). How to find the inertia tensor (or other mass properties) of a 3D solid body represented by a triangle mesh. Internal document at: [http:// number-one.com/blow/inertia/bb_inertia.doc](http://number-one.com/blow/inertia/bb_inertia.doc) [2017].
- Matas, G., Lantada, N., Corominas, J. , Gili, J.A., Ruiz-Carulla, R., Prades, A. (2017). RockGIS: A GIS-based model for the analysis of fragmentation in rockfalls. *Landslides*, Vol. 14, No. 5, pp. 1565-1578. DOI. 10.1007/s10346-017-0818-7.
- Niethammer, U., James, M. R., Rothmund, S., Travelletti, J., Joswig, M. (2012). UAV-Based Remote Sensing of the Super-Sauze Landslide: Evaluation and Results. *Engineering Geology*, Vol. 128. <https://doi.org/10.1016/j.enggeo.2011.03.012>.
- Prades, A., Matas, G., Núñez-Andrés, M.A., Buill, F., Lantada, N., Corominas, J. (2017). Determinación de trayectorias de bloques rocosos en ensayos mediante videogrametría. In: *Primer Congreso en Ingeniería Geomática*. Valencia (Spain), July 2017
- Stumpf, A., Malet, J.P., Kerle, N., Niethammer, U., Rothmund, S. (2013). Image-Based Mapping of Surface Fissures for the Investigation of Landslide Dynamics. *Geomorphology*, Vol. 186. <https://doi.org/10.1016/j.geomorph.2012.12.010>.
- Thoeni, K., Giacomini, A., Murtagh, R., Kniest, E. (2014). A comparison of multi-view 3d reconstruction of a rock wall using several cameras and a laser scanner. *The International Archives of the Photogrammetry, Remote Sensing and Spatial Information Sciences*, Vol. XL-5. ISPRS Technical Commission V Symposium, Riva del Garda, Italy, pp. 573-580.
- Tziavou, O., Pytharouli, S., Souter, J. (2018). Unmanned Aerial Vehicle (UAV) Based Mapping in Engineering Geological Surveys: Considerations for Optimum Results. *Engineering Geology*, Vol. 232, pp. 12–21. <https://doi.org/10.1016/j.enggeo.2017.11.004>.